Role and mechanism underlying FoxO6 in skeletal muscle *in vitro* and *in vivo*

LEI ZHANG[1,2], YIYI ZHANG[1,2], MIN ZHOU[1,2], SHUANG WANG[1,2], TIANE LI[1,2], ZHANGYONG HU[3*] and CHENGWU JIN[4*]

[1]Department of Endocrinology, Sichuan Provincial People's Hospital, University of Electronic Science and Technology of China; [2]Chinese Academy of Sciences Sichuan Translational Medicine Research Hospital, Chengdu, Sichuan 610072; [3]Department of Infection Disease, The First Affiliated Hospital of Chengdu Medical College, Chengdu, Sichuan 610041; [4]Department of General Surgery, Chengdu Fifth People's Hospital, The Fifth People's Hospital Affiliated with Chengdu University of Traditional Chinese Medicine, Chengdu, Sichuan 611130, P.R. China

Received June 30, 2020; Accepted December 15, 2020

DOI: 10.3892/ijmm.2021.4976

Abstract. Skeletal muscle atrophy is a common feature of patients suffering with chronic infection and other systemic diseases, including acquired immunodeficiency syndrome, chronic kidney disease and cancer. Therefore, understanding the molecular basis of muscle loss is of importance. The majority of members of the forkhead box O (FoxO) family can induce skeletal muscle atrophy; however, the effect of FoxO6 on skeletal muscle is not completely understood. The present study investigated the role of FoxO6 *in vitro* and *in vivo*. Compared with the small interfering RNA (si)-negative control (NC) group, C_2C_{12} cell proliferation (Cell Counting Kit-8 assay), myotube differentiation and myotube production were significantly decreased by FoxO6 knockdown, which was different from the known functions of other FoxO members. The immunofluorescence assay results demonstrated that si-FoxO6 clearly downregulated the expression levels of myosin heavy chain (MyHC) in C_2C_{12} myotubes compared with si-NC. The western blotting results indicated that compared with the si-NC group, FoxO6 knockdown induced C_2C_{12} myotube atrophy by notably downregulating myoblast determination protein 1 (MyoD), mTOR and MyHC expression levels, and by markedly upregulating ubiquitin ligase (atrogin1) and muscle RING-finger protein-1 (MURF1) expression levels. Similarly, in an *in vitro* model of TNF-α-induced myotube atrophy, the western blotting results indicated that FoxO6 expression levels were decreased, whereas atrogin1, MURF1, FoxO1 and FoxO3a expression levels were increased compared with the control group. Therefore, the results indicated that, unlike FoxO1 or FoxO3a, FoxO6 maintained C_2C_{12} myotubes and protected against atrophy. Consistent with the *in vitro* data, similar results were observed *in vivo*. Collectively, the results of the present study suggested that FoxO6 served a critical role in muscle cell metabolism *in vitro* and *in vivo*, and might serve as a promising therapeutic target for ameliorating skeletal muscle atrophy.

Correspondence to: Professor Chengwu Jin, Department of General Surgery, Chengdu Fifth People's Hospital, The Fifth People's Hospital Affiliated with Chengdu University of Traditional Chinese Medicine, 33 Mashi Street, Wenjiang, Chengdu, Sichuan 611130, P.R. China
E-mail: 285682577@qq.com

Professor Zhangyong Hu, Department of Infection Disease, The First Affiliated Hospital of Chengdu Medical College, 278 Middle Section of Baoguang Avenue, Xindu, Chengdu, Sichuan 610041, P.R. China
E-mail: chendu47@163.com

*Contributed equally

Key words: skeletal muscle atrophy, forkhead box O6, C_2C_{12}, atrogin1, muscle RING-finger protein-1

Introduction

Skeletal muscle atrophy is a debilitating response to chronic infection and other systemic diseases, including acquired immunodeficiency syndrome, tuberculosis, cancer, chronic obstructive pulmonary disease and chronic kidney disease (1). Skeletal muscle atrophy is characterized by muscle wasting and partial or complete loss of muscle function, which becomes more pronounced as the disease progresses (1-3). Several categories of drugs, including statins, antiviral therapies and immunosuppressants (e.g., glucocorticoids), cause muscle atrophy (4,5). Skeletal muscle atrophy severely affects quality of life, and current therapies display limited effects (6). Therefore, investigating the pathogenic mechanism underlying muscle atrophy and identifying effective therapeutic targets is of significant importance.

Jagoe *et al* (7,8) confirmed that under atrophic conditions, protein degradation rates in muscles were increased primarily via activation of the atrophy program. Muscle-specific

expression of atrogin1 and muscle RING-finger protein-1 (MURF1) is dramatically induced during atrophy (9,10). Additionally, the levels of several proteins are often markedly decreased in atrophying muscles, including myoblast determination protein 1 (MyoD), myosin heavy chain (MyHC) and mTOR, which have been reported to serve critical roles in muscle metabolism and are used as biomarkers (11-13).

Forkhead box O (FoxO) genes belong to the forkhead box gene family of transcription factors that contain the forkhead domain (14). In mammals, four FoxO genes have been identified: FoxO1, FoxO3a, FoxO4 and FoxO6 (15-17). Previous studies have demonstrated that FoxO genes are associated with cellular processes, including metabolism, the cell cycle, apoptosis and cellular homeostasis, and mediate cell responses to oxidative stress and antitumor drug treatment (14-18). The roles of other members of the FoxO family, including FoxO1, FoxO3 and FoxO4, in the regulation of skeletal muscle mass have been demonstrated in several studies (19,20). FoxO1 or FoxO3a overexpression in muscle is sufficient to induce skeletal muscle atrophy *in vivo* (21-24). Moreover, FoxO4 is necessary for TNF-induced atrogin1 expression (25).

FoxO6 is the most recently identified FoxO-encoding gene (17). In mammals, FoxO6 was initially observed in the central nervous system and was then reported to be ubiquitously expressed in various tissues, with higher expression levels in tissues undergoing oxidative stress (17). In the hippocampus, FoxO6 is negatively regulated by insulin/insulin like growth factor 1 signaling via the PI3K/AKT signaling pathway (26,27). Additionally, in muscles undergoing oxidative stress, FoxO6 can form a regulatory loop with peroxisome proliferator-activated receptor γ coactivator 1-α (PGC-1α) to establish the level of oxidative metabolism (28). In 2018, Sun *et al* (29) reported that FoxO6 controls the growth of the craniofacial complex via the Hippo signaling pathway. However, the effects of FoxO6 on skeletal muscle atrophy are not completely understood.

The present study investigated the role of FoxO6 in maintaining the proliferation and differentiation of skeletal muscle, as well as the underlying mechanism, *in vitro and in vivo*.

Materials and methods

Reagents and antibodies. The primary antibodies targeted against mTOR (cat. no. 2983) and β-actin (cat. no. 4970) were purchased from Cell Signaling Technology, Inc. The primary antibodies targeted against FoxO6 (cat. no. 19122-1-AP) and MURF1 (cat. no. 55456-1-AP) were purchased from ProteinTech Group, Inc. The primary antibodies targeted against atrogin1 (cat. no. ab168372), MyoD (cat. no. ab203383), FoxO3a (cat. no. ab70315), FoxO1 (cat. no. ab52857) and MyHC (cat. no. ab11083) were purchased from Abcam. Anti-mouse (cat. no. 7076) and anti-rabbit (cat. no. 7074) IgG HRP-conjugated antibodies were purchased from Cell Signaling Technology, Inc. TNF-α (cat. no. AF-315-01A) was acquired from PeproTech EC Ltd. Phalloidin (cat. no. P5282) was purchased from Sigma-Aldrich (Merck KGaA). Goat anti-mouse IgG (H+L) Cross-Adsorbed secondary antibody, Alexa Fluor (488; cat. no. A11001) were purchased from Thermo Fisher Scientific, Inc. Cell Counting Kit-8 (cat. no. CK04) and DAPI (cat. no. D212) were purchased from Dojindo Molecular Technologies, Inc. Horse serum (cat. no. BL209A; Beijing Lanjieke Technology Co., Ltd.). Control small interfering RNA [si; si-negative control (NC)] and FoxO6-specific siRNAs were purchased from Beijing Viewsolid Biotech Co., Ltd. GenMute siRNA transfection reagent (cat. no. SL100568) was from SignaGen Laboratories.

Cell line and culture. The murine myoblast cell line C_2C_{12} (The Cell Bank of Type Culture Collection of Chinese Academy of Sciences) was used within the first 10 passages. Cells were cultured in DMEM (Gibco; Thermo Fisher Scientific, Inc.) supplemented with 10% FBS (Biowest), 100 U/ml penicillin and 100 uU/ml streptomycin in a humidified atmosphere with 5% CO_2 at 37˚C. To obtain C_2C_{12} myotubes, C_2C_{12} cells were differentiated in DMEM/2% horse serum for 10 days in a humidified atmosphere with 5% CO_2 at 37˚C, changing the medium every 2 days. The mouse hepatocyte cell line AML12 was purchased from The Cell Bank of Type Culture Collection of Chinese Academy of Sciences and cultured in DMEM supplemented with 10% FBS, 40 ng/ml dexamethasone (cat. no. BS134A; Biosharp Life Sciences), and 1% insulin, transferrin and selenium (Invitrogen; Thermo Fisher Scientific, Inc.) in a humidified atmosphere with 5% CO_2 at 37˚C. For the muscle atrophy model *in vitro*, C_2C_{12} myotubes were treated with TNF-α (50 ng/ml) for 6 h with 5% CO_2 at 37˚C.

Cell proliferation assay. Relative cell proliferation of si-FoxO6-treated C_2C_{12} cells was determined using the CCK-8 kit. Cells were seeded ($3x10^3$/well) into 96-well plates and transfection with si-NC (50 nM) or si-FoxO6-3 (50 nM) was performed for 24, 48, 72, 96 or 120 h at room temperature using GenMute siRNA transfection reagent according to the manufacturer's protocol. Following removal of the culture medium, 100 μl medium and 10 μl CCK-8 reagent were added to each well and incubated for 3 h at 37˚C in the dark. Absorbance was measured at a wavelength of 450 nm using a microplate reader (Thermo Fisher Scientific, Inc.). The assay was performed in triplicate.

Western blotting. Mouse muscle tissues were ground in liquid nitrogen. Total protein was extracted from tissues and cells using M-PER Mammalian Protein Extraction Reagent (cat. no. 78503; Pierce; Thermo Fisher Scientific, Inc.). For mouse muscle tissues, 1% SDS lysis reagent (cat. P0013G; Beyotime Institute of Biotechnology) was also used for protein extraction. Protein concentrations of cell and tissue lysates were quantified using a Qubit Protein Assay kit (cat. no. 2157145; Invitrogen; Thermo Fisher Scientific, Inc.) and a Qubit 2.0 fluorometer (Thermo Fisher Scientific, Inc.) according to the manufacturer's instructions. Equal amounts of protein (30 μg) were separated via 8 or 10% SDS-PAGE and transferred to PVDF membranes (EMD Millipore). Following blocking 5% skimmed milk at 37˚C for 2 h, the membranes were incubated overnight at 4˚C with the following primary antibodies: Anti-MyoD (1:800), anti-β-actin (1:1,000), anti-MyHC (1:1,000), anti-mTOR (1:2,000), anti-FoxO6 (1:1,000), anti-FoxO3a (1:2,000), anti-FoxO1 (1:1,000), anti-MURF1 (1:1,000) and anti-atrogin1 (1:2,000). After washing in TBST (1% Tween-20), the membranes were incubated with secondary antibodies (1:2,000) at 37˚C for 2 h. Protein bands

were visualized using enhanced chemiluminescence reagents (Amersham; Cytiva). β-actin was used as the loading control.

FoxO6 knockdown. C_2C_{12} cells were plated at a density of $1.5x10^5$/well and grown overnight. Subsequently, cells were transfected with 50 nM si-FOXO6-1, si-FOXO6-2, si-FOXO6-3 or si-NC using GenMute transfection reagent (cat. no. SL100568) at room temperature according to the manufacturer's protocol. At 48 h post-transfection, cells were lysed using TRIzol® reagent for RNA extraction (Invitrogen; Thermo Fisher Scientific, Inc.) and M-PER Mammalian Protein Extraction Reagent (cat. no. 78503; Pierce; Thermo Fisher Scientific, Inc.) for protein extraction. Subsequently, transfection efficiency was assessed via reverse transcription-quantitative PCR (RT-qPCR) and western blotting. siRNA oligomers were designed and synthesized by Beijing Viewsolid Biotech Co., Ltd (China), as follows: si-FoxO6-1 forward, 5'-GGUCGGACCCUUGCGGAAATTdTdT-3' and reverse, 3'-dTdTUUUCCGCAAGGGUCCGACCTT-5'; si-FoxO6-2 forward, 5'-GGCACUGGCAAGAGUUCAUTT dTdT-3' and reverse, 3'-dTdTAUGAACUCUUGCCAGUG CCTT-5'; and si-FoxO6-3 forward, 5'CCAUCAUCCUCAACG ACUUTTdTdT-3' and reverse, 3'-dTdTAAGUCGUUGAG GAUGAUGGTT-5'. The scrambled NC siRNA (si-NC) was purchased from Beijing Viewsolid Biotech Co., Ltd.

RT-qPCR. Total RNA from cells and tissues was extracted using TRIzol. RT-qPCR was performed according to the manufacturer's protocol. Briefly, total RNA was reverse transcribed into cDNA using PrimeScript™ RT Master Mix (Perfect Real Time; cat. no. RR036A; Takara Bio, Inc.). Subsequently, qPCR was performed using SYBR Premix Ex Taq II (cat. no. RR820A; Takara Bio, Inc.) and a CFX Connect instrument (Bio-Rad Laboratories, Inc.). The following primers were used for qPCR: Mouse FoxO6 forward, 5'-CAG CAACCCTCTTCGTTCACA-3' and reverse, 5'-CAGGAC TGGTTAAGATGGGAGACT-3' (101 bp); and mouse β-actin forward, 5'-AGATTACTGCTCTGGCTCCTAGC-3' and reverse, 5'-ACTCATCGTACTCCTGCTTGCT-3' (147 bp). The following thermocycling conditions were used for qPCR: 95˚C for 30 sec; 40 cycles of 5 sec at 95˚C and 30 sec at 56˚C; and melting curve analysis. mRNA expression levels were quantified using the $2^{-\Delta\Delta Cq}$ method (30) and normalized to the internal reference gene β-actin using CFX Connect instrument software (CFX Maestro 2.0; Bio-Rad Laboratories, Inc.). RT-qPCR was performed in duplicate.

Myotube diameter assay. At 48 h post-transfection, C_2C_{12} cells were treated with differentiation medium for 10 days. The differentiation medium was changed every 2 days. Subsequently, myotubes were fixed in 4% polyformaldehyde at room temperature for 30 min, then stained with 50 μg/ml fluorescent phalloidin conjugate solution in PBS for 40 min at room temperature. Stained myotubes were observed using a Ti2 inverted fluorescence microscope (Nikon Corporation; magnification, x20) and analyzed using NIS-Elements BR Analysis software (version 5.20.02; Nikon Instruments, Inc.).

Immunofluorescence staining. C_2C_{12} myotubes cultured in 6-well plates ($1.5x10^5$/well) were fixed with 4% paraformaldehyde at room temperature for 20 min, permeabilised with 0.5% Triton X-100 for 20 min at 37˚C and blocked in PBS buffer containing 5% BSA (cat. no. A8020; Beijing Solarbio Science & Technology Co., Ltd.) at 4˚C overnight. Cells were incubated with anti-MyHC (1:4,000) overnight at 4˚C. Subsequently, cells were incubated with a goat anti-mouse fluorescein-conjugated Alexa Fluor 488 antibody (1:1,000) for 1.5 h at room temperature. Cell nuclei were stained with DAPI for 10 min. Stained cells were visualized using a Ti2 inverted fluorescence microscope (Nikon Corporation; magnification, x20) and analyzed using NIS-Elements BR Analysis software (version 5.20.02; Nikon Instruments, Inc.).

Animals. A total of 16 6-week-old healthy male C57BL/6J mice (weight, 16-18 g) and five 8-week-old (weight, 20-22 g) healthy male C57BL/6J mice were purchased from Beijing Vital River Laboratory Animal Technology Co., Ltd. All animals were subjected to equivalent feeding conditions. Mice were housed at a constant temperature (22-24˚C) with humidity (50-60%), 12-h light/dark cycles and *ad libitum* access to water and food. In the present study, for the measurement of FoxO6 mRNA and protein expression levels, the 8-week-old healthy male C57BL/6J mice were used to obtain liver, heart, lung, colon and skeletal muscle tissues, respectively. The 16 6-week-old healthy male C57BL/6J mice were used for the AAV9-siRNA knockdown experiment. According to the siRNA knockdown efficiency *in vitro*, adeno-associated virus 9 (AAV9)-shFoxO6 (based on the si-FOXO6-3 sequence) was prepared. Control AAV9 (shRNA-scramble) and AAV9-shFoxO6 particles were packaged, purified and titrated by ViGene Biosciences, Inc. For preliminary experiments, six six-week-old healthy male C57BL/6J mice were used to verify the efficiency of AAV9-shFoxO6 transfection into skeletal muscles (n=3 per group; control AAV9=3 and AAV9-shFoxO6=3). For subsequent experiments, 50 μl AAV9 ($1x10^{11}$ genome copies) carrying control AAV9 (n=5) or AAV9-shFoxO6 (n=5) was injected into the skeletal muscles. After 4 weeks, except for slightly reduced activity of AAV9-shFoxO6 mice, no obvious abnormalities, such as diet or drinking water, were observed. Subsequently, AAV9-shFoxO6 mice and control AAV9 mice were euthanized by the intraperitoneal injection of 150 mg/kg sodium pentobarbital. Skeletal muscles were collected and stored at -80˚C until further analysis.

Statistical analysis. Statistical analyses were performed using GraphPad Prism software (version 6; GraphPad Software, Inc.). Data are presented as the mean ± SEM from three independent experiments. SPSS (version 21.0; IBM Corp.) software was used to assess the normal distribution and homogeneity of variances of the data using the Shapiro-Wilk test and the Levene test. Comparisons between two groups were analyzed using the unpaired Student's t-test. Comparisons between multiple groups were analyzed using one-way ANOVA followed by Dunnett's post-hoc test. $P<0.05$ was considered to indicate a statistically significant difference.

Results

FoxO6 is highly expressed in skeletal muscle cells. Among the FoxO family members, FoxO1, FoxO3a, and FoxO4 are

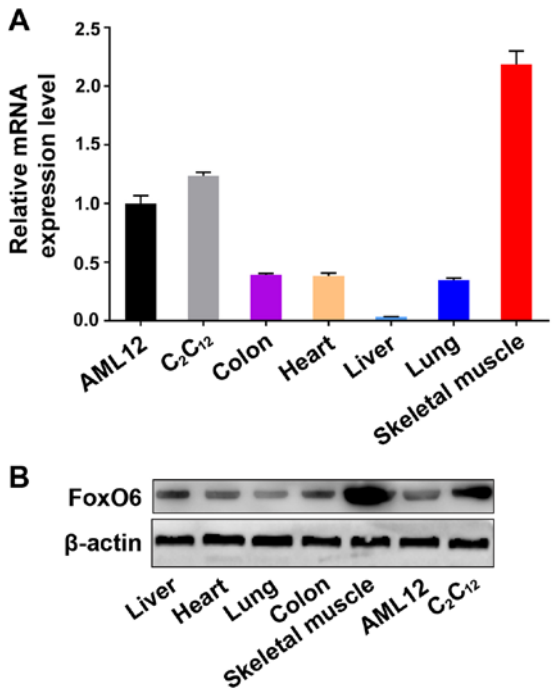

Figure 1. FoxO6 expression in mouse cell lines and tissues. FoxO6 (A) mRNA and (B) protein expression levels were measured via reverse transcription-quantitative PCR and western blotting, respectively. FoxO6, forkhead box O6.

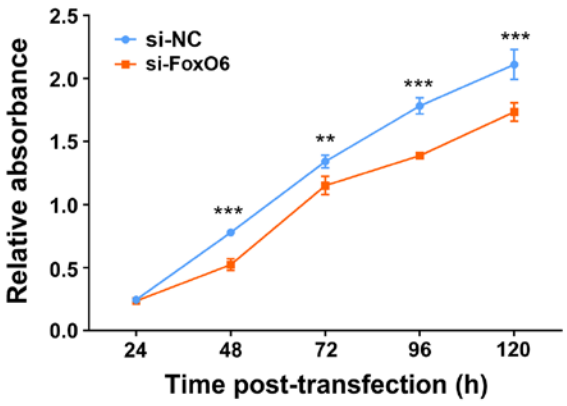

Figure 2. FoxO6 knockdown significantly inhibits C_2C_{12} myoblast cell proliferation. At 24 h post-transfection, C_2C_{12} cell proliferation was assessed by performing the Cell Counting Kit-8 assay. Data are presented as the mean ± SEM from three independent experiments performed in triplicate. **P<0.01 and ***P<0.001 vs. si-FoxO6. si-FoxO6, si-FoxO6-3; FoxO6, forkhead box O6; si, small interfering RNA; NC, negative control.

expressed in almost all tissues (14-16). The present study measured FoxO6 mRNA and protein expression levels in the major tissues of five 8-week-old (weight, 20-22 g) healthy male C57BL/6J mice and in cell lines by performing RT-qPCR and western blotting, respectively. The investigated samples included the following: Mouse liver, mouse heart, mouse lung, mouse colon and mouse skeletal muscle obtained from healthy mice, C_2C_{12} cells and AML12 cells. FoxO6 was expressed in the cell lines and tissues, especially in mouse skeletal muscle tissues and the C_2C_{12} myoblast cell line (Fig. 1), which suggested that FoxO6 might be essential for maintaining the structure and function of muscle.

Efficient FoxO6 knockdown using siRNA. To determine whether FoxO6 served a key role in muscle metabolism, three siRNA oligomer screening assays in C_2C_{12} myoblast cells were designed as follows: si-FoxO6-1 forward, 5'-GGUCGGACCCUUGCGGAAATTdTdT-3' and reverse, 3'-dTdTUUUCCGCAAGGGUCCGACCTT-5'; si-FoxO6-2 forward, 5'-GGCACUGGCAAGAGUUCAUTTdTdT-3' and reverse, 3'-dTdTAUGAACUCUUGCCAGUGCCTT-5'; and si-FoxO6-3 forward, 5'CCAUCAUCCUCAACGACUUTTdTdT-3' and reverse, 3'-dTdTAAGUCGUUGAGGAUGAUGGTT-5'. To identify the most efficient si-FoxO6 oligomer, in the initial screen, C_2C_{12} cells were transfected with one of the three si-FoxO6 oligomers or the si-NC oligomer for 48 h. Subsequently, cells were lysed, and then RNA and protein expression levels were determined via RT-qPCR and western blotting, respectively. According to the RT-qPCR results, the oligomer that most significantly knocked down FoxO6 expression levels compared with the si-NC group was si-FoxO6-3, and similar results were obtained by western blotting (Fig. S1). Therefore, si-FoxO6-3 was used for subsequent experiments.

C_2C_{12} myoblast cell proliferation is decreased by FoxO6 knockdown. The aforementioned results suggested that high FoxO6 expression in mouse skeletal muscle and C_2C_{12} myoblast cells might be related to the structure and function of muscle. To determine whether FoxO6 was necessary for myoblast cell proliferation, si-FoxO6 oligomer was transfected into C_2C_{12} myoblast cells to assess the effect of FoxO6 knockdown on cell proliferation by performing the CCK-8 assay. The results demonstrated that compared with the si-NC group, cell proliferation was significantly inhibited by FoxO6 knockdown at 48, 72, 96 and 120 h post-transfection (Fig. 2).

FoxO6 knockdown inhibits C_2C_{12} myotube differentiation. The results demonstrated that FoxO6 was highly expressed in muscle at the RNA and protein levels, and FoxO6 knockdown significantly inhibited C_2C_{12} cell proliferation compared with the si-NC group. Moreover, the results indicated that FoxO6 knockdown inhibited myotube differentiation, as morphologically demonstrated by the significantly decreased diameter of differentiated C_2C_{12} myotubes in the si-FoxO6 group compared with the si-NC group (Fig. 3A and B). In addition, the immunofluorescence assay results indicated that FoxO6 knockdown notably decreased the number of myotubes expressing MyHC compared with the si-NC group (Figs. 3C and S2).

Furthermore, to investigate the possible mechanism underlying FoxO6-maintained myotube activity, the protein expression levels of several critical biomarkers involved in muscle metabolism, including MyoD, MyHC, mTOR, atrogin1 and MURF1, were determined via western blotting. In differentiated C_2C_{12} myotubes, FoxO6 was knocked down using siRNA for 48 h. Compared with the si-NC group, FoxO6 knockdown markedly downregulated FoxO6, mTOR, MyHC and MyoD expression levels, but notably upregulated atrogin1 and MURF1 expression levels (Fig. 3C). Collectively, the results suggested that FoxO6 was required for myotube differentiation and maintenance in C_2C_{12} cells.

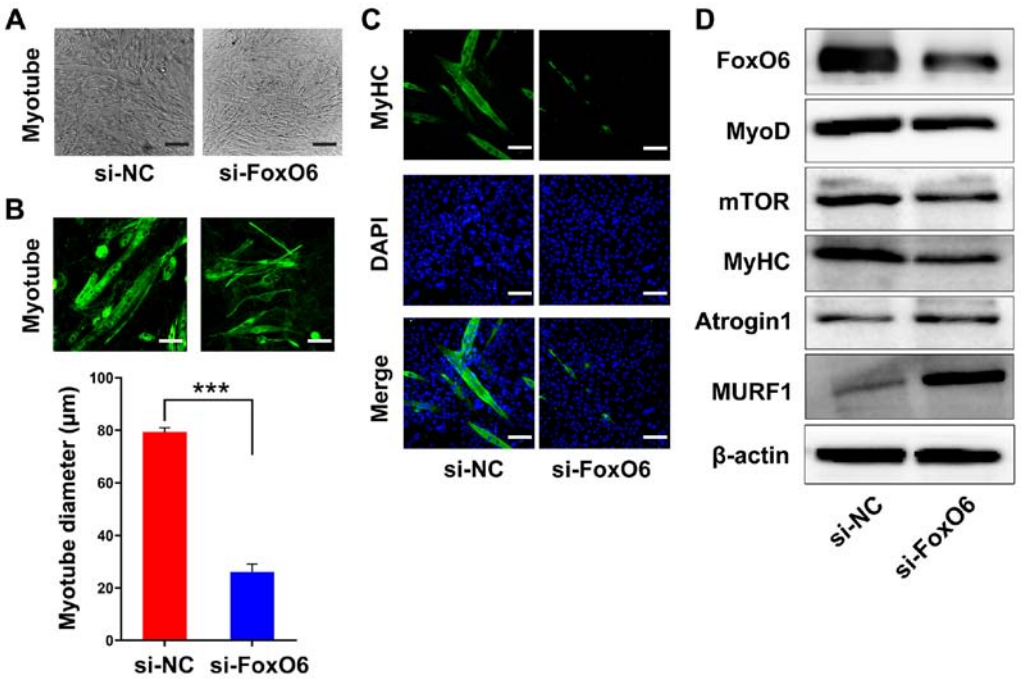

Figure 3. FoxO6 knockdown inhibits C_2C_{12} myotube differentiation. (A) Representative photographs of C_2C_{12} myotubes in the si-NC and si-FoxO6 groups. (B) Myotube morphology was assessed using FITC-labeled phalloidin and myotube diameters were measured. (C) MyHC expression in FoxO6-knockdown C_2C_{12} myotubes was assessed by conducting immunofluorescence staining. (D) Expression levels of muscle-related proteins in FoxO6-knockdown C_2C_{12} myotubes were examined via western blotting. β-actin was used as the loading control. All scale bars, 100 μm. ***P<0.001. FoxO6, forkhead box O6; si, small interfering RNA; NC, negative control; MyHC, myosin heavy chain; MyoD, myoblast determination protein 1; MURF1, muscle RING-finger protein-1.

FoxO6 is downregulated in TNF-α-induced C_2C_{12} myotube atrophy. To further verify the aforementioned results, an *in vitro* model of TNF-α-induced myotube atrophy, which has been proven valid by Eley and Chen (31,32), was utilized. Atrogin1 and MURF1 expression levels were markedly upregulated in atrophied C_2C_{12} myotubes compared with the control group (Fig. 4). Furthermore, FoxO6 expression levels were notably downregulated, but FoxO1 and FoxO3a expression levels were markedly upregulated in atrophied C_2C_{12} myotubes compared with the control group. In other words, the results indicated that, unlike FoxO1 or FoxO3a, FoxO6 was required for the maintenance of C_2C_{12} myotubes. The aforementioned results indicated that FoxO6 regulated C_2C_{12} myotubes in an *in vitro* model of TNF-α-induced myotube atrophy.

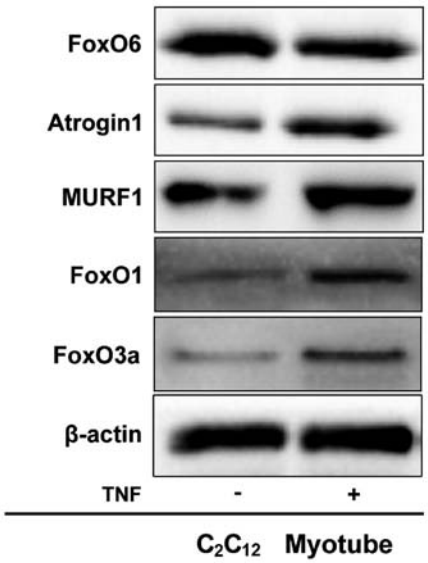

Figure 4. Muscle-related protein expression levels in atrophic C_2C_{12} myotubes. To model muscle atrophy, C_2C_{12} myotubes were treated with TNF-α (50 ng/ml) for 6 h with 5% CO_2 at 37˚C. Subsequently, the expression levels of several muscle-related proteins were determined via western blotting. β-actin was used as the loading control. FoxO, forkhead box O; MURF1, muscle RING-finger protein-1.

FoxO6 knockdown causes myofiber atrophy in mice. The aforementioned results indicated that FoxO6 served a key role in maintaining C_2C_{12} myotubes *in vitro*. Compared with the si-NC group, FoxO6 knockdown induced the downregulation of major muscle proteins, including MyoD, MyHC and mTOR, and the upregulation of ubiquitin ligase (atrogin1) and MURF1. Therefore, whether AAV9-shFoxO6 resulted in skeletal muscle fiber atrophy *in vivo* was investigated. According to the knockdown efficiency of siFoxO6-3 *in vitro*, AAV9-shFoxO6 (based on the siFoxO6-3 sequence) was prepared. AAV9-control (control group; n=5) or AAV9-shFoxO6 (knockdown group; n=5) was injected into the skeletal muscles of each mouse. At 4 weeks post-injection, FoxO6 RNA expression levels were significantly decreased by 65% in the AAV9-Ctrl group compared with the AAV9-shFoxO6 group (Fig. S3). Subsequently, the protein expression levels of atrogin1 and MURF1 in myofibers of AAV9-control or AAV9-shFoxO6 mice were measured. Atrogin1 and MURF1 expression levels were significantly increased in AAV9-shFoxO6 mice compared with AAV9-control mice (Fig. 5). Moreover, the expression levels of MyoD, MyHC and mTOR were significantly decreased in AAV9-shFoxO6 mice compared with AAV9-control mice. Thus, the results suggested that FoxO6

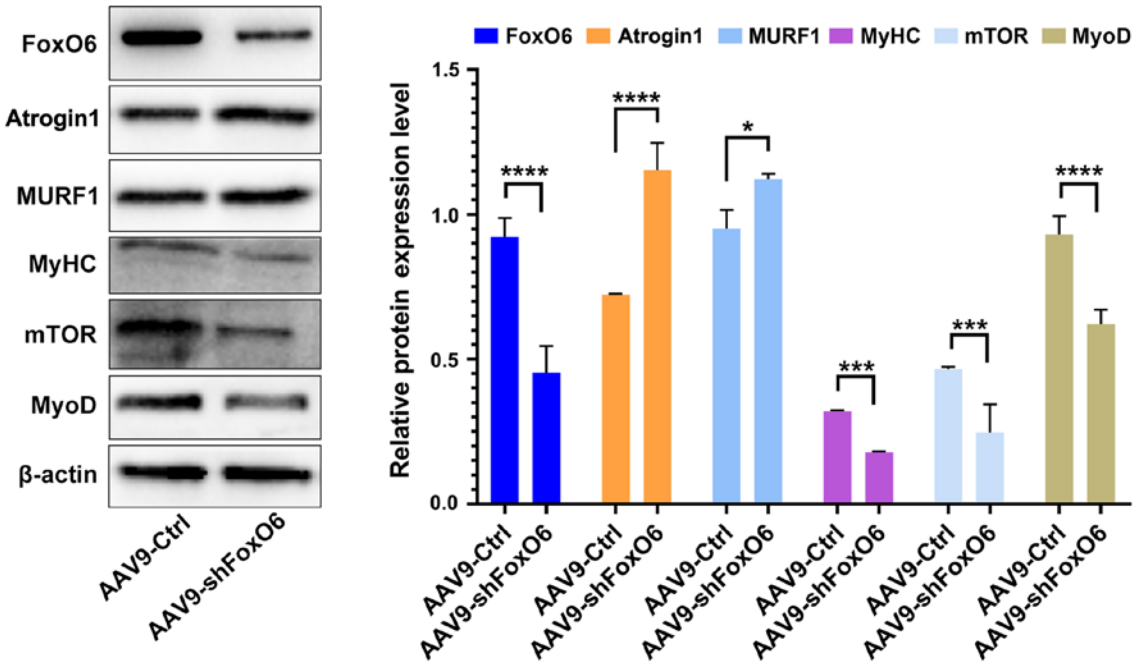

Figure 5. Muscle-related protein expression levels in skeletal muscles of AAV9-shFoxO6-treated mice. Protein expression levels were determined via western blotting. β-actin was used as the loading control. *P<0.05, ***P<0.001 and ****P<0.0001. AAV9, adeno-associated virus 9; sh, short hairpin; FoxO, forkhead box O; si, small interfering RNA; MURF1, muscle RING-finger protein-1; MyHC, myosin heavy chain; MyoD, myoblast determination protein 1; AAV9-Ctrl, AAV9 control group.

knockdown induced myofiber atrophy. Collectively, the results of the present study indicated that FoxO6 prevented skeletal muscle atrophy and was required for muscle activity.

Discussion

Skeletal muscle atrophy is one of the major characteristics of patients with chronic disease, and the associated muscle loss becomes more pronounced as the disease progresses (1-3,20). Several categories of drugs, including statins, antiviral therapies and immunosuppressants, also cause muscle atrophy (4,5). Although significant progress has been made towards understanding skeletal muscle loss, the relevant molecules and underlying cellular mechanisms are not completely understood.

Previous studies have demonstrated that the majority of members of the FoxO family are associated with the regulation of skeletal muscle metabolism (19,20). In muscle, FoxO1 or FoxO3a could induce skeletal muscle atrophy *in vivo* (21,22,24). FoxO4 was also involved in the physiological regulation of mammalian skeletal muscle hypertrophy and atrophy (20,33). In C_2C_{12} myotubes, Moylan *et al* (25) reported that the TNF-induced atrogin1 expression was dependent on FoxO4 expression, but not on FoxO1/3 signaling. Chung *et al* (28) also demonstrated that FoxO6 could form a regulatory loop with PGC-1α to establish the level oxidative metabolism in muscles undergoing oxidative stress. However, as the most recently discovered FoxO family member, the functions and exact mechanism underlying FoxO6 in skeletal muscle metabolism are not completely understood.

The present study investigated the role of FoxO6 *in vitro* with si-FoxO6 and *in vivo* with AAV9-shFoxO6. FoxO6 expression levels in several samples, including samples of mouse liver, heart, lung, colon and skeletal muscle, as well as the C_2C_{12} and AML12 cell lines, were assessed. FoxO6 expression was particularly high in mouse skeletal muscles and C_2C_{12} myoblast cells. To assess the hypothesis that FoxO6 might serve as an important regulator in the maintenance of skeletal muscle function, the effect of FoxO6 knockdown on C_2C_{12} cell proliferation was investigated. Compared with the si-NC group, FoxO6 knockdown significantly inhibited C_2C_{12} cell proliferation. Furthermore, C_2C_{12} myotubes were used to verify whether si-FoxO6 resulted in myotube atrophy. The morphological characteristics were examined, and a significant decrease in myotube diameter was observed following FoxO6 knockdown compared with the si-NC group. Moreover, as the major component of skeletal muscle (13,34,35), MyHC expression was analyzed via immunofluorescence staining. The results demonstrated that FoxO6 knockdown notably downregulated the expression level of MyHC in myotubes compared with the si-NC group. Collectively, the results of the present study suggested that FoxO6 might be required for C_2C_{12} myotube differentiation and maintenance.

Skeletal muscle mass is essential for motility, whole body metabolism and viability. Patients suffering from muscle atrophy often become weaker and unable to perform normal activities, and in severe cases, muscle atrophy can result in death. The primary characteristics of patients suffering from muscle atrophy are extreme thinness and wasting. Under poor conditions, muscle-related proteins are often severely degraded (1-3,6). Consistent with the important role of FoxO1 or FoxO3a during muscle atrophy, the aforementioned FoxO6 knockdown-mediated effects were noted in atrophic C_2C_{12} myotubes. Interestingly, the results of the present study suggested that, unlike FoxO1 or FoxO3a, FoxO6 protected C_2C_{12} myotubes against atrophy.

Increasing evidence has demonstrated that the loss of muscle proteins in skeletal muscle leads to severe myopathy, which in turn leads to a series of muscular disorders associated with muscle protein dysfunction (11-13,36). The expression of muscle proteins is significantly reduced when skeletal muscle atrophy occurs (34,35). Therefore, to investigate the possible mechanism underlying FoxO6-induced maintenance of myotube activity, the present study assessed several critical biomarkers in muscle, including MyoD, MyHC and mTOR, via western blotting. Under several conditions, including fasting, a variety of diseases (e.g., cancer, diabetes mellitus and Cushing's Syndrome) and in specific muscles upon denervation or disuse, muscle atrophy participates in a common mechanism that upregulates atrogin1 and MURF1 (1,7,9,10). In the present study, compared with the si-NC group, FoxO6 knockdown notably downregulated mTOR, MyHC and MyoD expression levels, and markedly upregulated atrogin1 and MURF1 expression levels in C_2C_{12} myotubes. Additionally, an *in vitro* model of TNF-α-induced myotube atrophy was utilized. Similar results were obtained in the *in vitro* model. For example, FoxO6 expression levels were notably downregulated, and atrogin1 and MURF1 expression levels were markedly upregulated in atrophied C_2C_{12} myotubes compared with the control group. The results also demonstrated that FoxO1 and FoxO3a expression levels were notably upregulated in atrophied C_2C_{12} myotubes compared with the control group. In other words, the results indicated that FoxO6 maintained C_2C_{12} myotubes and protected against atrophy, which was different from the known functions of FoxO1 or FoxO3a.

Consistent with the *in vitro* results, similar results were also obtained *in vivo*. Atrogin1 and MURF1 expression levels were significantly increased in skeletal muscles isolated from AAV9-shFoxO6 mice compared with AAV9-control mice. Moreover, MyoD, MyHC and mTOR expression levels were notably decreased in AAV9-shFoxO6 mice compared with AAV9-control mice. In conclusion, the results of the present study indicated that FoxO6 was required for maintaining C_2C_{12} myotubes and protecting against atrophy *in vitro* and *in vivo*; thus, the present study highlighted the protective effects of FoxO6 in muscle protein metabolism.

Acknowledgements

The authors would like to thank Mr Guanyu Zhou (Chengdu University of Traditional Chinese Medicine) for assisting with the data analysis, and Mr Qiang Wang (Chengdu University of Traditional Chinese Medicine) and Ms Wanping Xia (Chengdu University of Traditional Chinese Medicine) for their valuable assistance in the animal experiments.

Funding

The present study was supported by the Sichuan Science and Technology Program (grant nos. 2020YFS0422, 2016JY0207, 2019YJ0150, 2019YFS0263, 2017FZ0091 and 2018RZ0091).

Availability of data and materials

The datasets used and/or analyzed during the current study are available from the corresponding author on reasonable request.

Authors' contributions

ZH and CJ contributed to the conceptualization of the study and acquisition of funding. LZ and CJ were involved in designing and performing the experiments. YZ, MZ and SW provided materials, and participated in performing the experiments and analyzing the data. LZ drafted the manuscript. ZH and CJ contributed to revising the manuscript. SW and TL performed the animal experiments and generated the figures. All authors are responsible for all aspects of the study in ensuring that questions relevant to the accuracy or integrity of any part of the study are appropriately investigated and resolved. All authors read and approved the final version of manuscript.

Ethics approval and consent to participate

All animal procedures were performed in accordance with the Guiding Opinions on the Good Treatment of Laboratory Animals (Sichuan Provincial Laboratory Animal Public Service Center) guidelines and were approved by the Institutional Animal Care and Treatment Committee of Sichuan Province (approval no. 2018328A), which was affiliated to Sichuan Academy of Medical Sciences & Sichuan Provincial People's Hospital.

Patient consent for publication

Not applicable.

Competing interests

The authors declare that they have no competing interests.

References

1. Sandri M: Autophagy in skeletal muscle. FEBS Lett 584: 1411-1416, 2010.
2. Lecker SH, Goldberg AL and Mitch WE: Protein degradation by the ubiquitin-proteasome pathway in normal and disease states. J Am Soc Nephrol 17: 1807-1819, 2006.
3. Lecker SH, Jagoe RT, Gilbert A, Gomes M, Baracos V, Bailey J, Price SR, Mitch WE and Goldberg AL: Multiple types of skeletal muscle atrophy involve a common program of changes in gene expression. FASEB J 18: 39-51, 2004.
4. Fappi A, de Carvalho Neves J, Sanches LN, Silva PV, Sikusawa GY, Brandão TPC, Chadi G and Zanoteli E: Skeletal muscle response to deflazacort, dexamethasone and methylprednisolone. Cells 8: 406, 2019.
5. Gupta A and Gupta Y: Glucocorticoid-Induced myopathy: Pathophysiology, diagnosis, and treatment. Indian J Endocrinol Metab 17: 913-916, 2013.
6. Cohen S, Nathan JA and Goldberg AL: Muscle wasting in disease: Molecular mechanisms and promising therapies. Nat Rev Drug Discov 14: 58-74, 2015.
7. Jagoe RT and Goldberg AL: What do we really know about the ubiquitin-proteasome pathway in muscle atrophy? Curr Opin Clin Nutr Metab 4: 183-190, 2001.
8. Jagoe RT, Lecker SH, Gomes M and Goldberg AL: Patterns of gene expression in atrophying skeletal muscles: The response to food deprivation. FASEB J 16: 1697-1712, 2002.
9. GomesMD, Lecker SH, Jagoe RT, Navon A and Goldberg AL: Atrogin-1, a muscle-specific F-box protein highly expressed during muscle atrophy. Proc Natl Acad Sci USA 98: 14440-14445, 2001.
10. Bodine SC, Latres E, Baumhueter S, Lai VK, Nunez L, Clarke BA, Poueymirou WT, Panaro FJ, Na E, Dharmarajan K, *et al*: Identification of ubiquitin ligases required for skeletal muscle atrophy. Science 294: 1704-1708, 2001.

11. Megeney LA, Kablar B, Garrett K, Anderson JE and Rudnicki MA: MyoD is required for myogenic stem cell function in adult skeletal muscle. Genes Dev 10: 1173-1183, 1996.
12. Bodine SC, Stitt TN, Gonzalez M, Kline WO, Stover GL, Bauerlein R, Zlotchenko E, Scrimgeour A, Lawrence JC, Glass DJ and Yancopoulos GD: Akt/mTOR pathway is a crucial regulator of skeletal muscle hypertrophy and can prevent muscle atrophy *in vivo*. Nat Cell Biol 3: 1014-1019, 2001.
13. Agbulut O, Noirez P, Beaumont F and Butler-Browne G: Myosin heavy chain isoforms in postnatal muscle development of mice. Biol Cell 95: 399-406, 2003.
14. Hannenhalli S and Kaestner KH: The evolution of fox genes and their role in development and disease. Nat Rev Genet 10: 233-240, 2009.
15. Link W: Introduction to FOXO biology. Methods Mol Biol 1890: 1-9, 2019.
16. Monsalve M and Olmos Y: The complex biology of FOXO. Curr Drug Targets 12: 1322-1350, 2011.
17. Jacobs FM, van der Heide LP, Wijchers PJ, Burbach JPH, Hoekman MFM and Smidt MP: FoxO6, a novel member of the foxo class of transcription factors with distinct shuttling dynamics. J Biol Chem 278: 35959-35967, 2003.
18. Liu W, Li Y and Luo B: Current perspective on the regulation of FOXO4 and its role in disease progression. Cell Mol Life Sci 77: 651-663, 2020.
19. Reed SA, Sandesara PB, Senf SM and Judge AR: Inhibition of FoxO transcriptional activity prevents muscle fiber atrophy during cachexia and induces hypertrophy. FASEB J 26: 987-1000, 2012.
20. Sandri M, Sandri C, Gilbert A, Skurk C, Calabria E, Picard A, Walsh K, Schiaffino S, Lecker SH and Goldberg AL: Foxo transcription factors induce the atrophy-related ubiquitin ligase atrogin-1 and cause skeletal muscle atrophy. Cell 117: 399-412, 2004.
21. Kamei Y, Miura S, Suzuki M, Kai Y, Mizukami J, Taniguchi T, Mochida K, Hata T, Matsuda J, Aburatani H, *et al*: Skeletal muscle FOXO1 (FKHR) transgenic mice have less skeletal muscle mass, down-regulated type I (slow twitch/red muscle) fiber genes, and impaired glycemic control. J Biol Chem 279: 41114-41123, 2004.
22. Xu J, Li RS, Workeneh B, Dong Y, Wang X and Zhaoyong Hu: Transcription factor FoxO1, the dominant mediator of muscle wasting in chronic kidney disease, is inhibited by microRNA-486. Kidney Int 82: 401-411, 2012.
23. Zhao J, Brault JJ, Schild A, Cao P, Sandri M, Schiaffino S, Lecker SH and Goldberg AL: FoxO3 coordinately activates protein degradation by the autophagic/lysosomal and proteasomal pathways in atrophying muscle cells. Cell Metabol 6: 472-483, 2007.
24. Mammucari C, Milan G, Romanello V, Masiero E, Rudolf R, Piccolo PD, Burden SJ, Lisi RD, Sandri C, Zhao JH, *et al*: Foxo3 controls autophagy in skeletal muscle *in vivo*. Cell Metabol 6: 458-471, 2007.
25. Moylan JS, Smith JD, Chambers MA, McLoughlin TJ and Reid MB: TNF induction of atrogin-1/MAFbx mRNA depends on Foxo4 expression but not AKT-Foxo1/3 signaling. Am J Physiol Cell Physiol 295: C986-C993, 2008.
26. Hoekman MF, Jacobs FM, Smidt MP and Burbach JP: Spatial and temporal expression of FoxO transcription factors in the developing and adult murine brain. Gene Expr Patterns 6: 134-140, 2006.
27. Salih DA, Rashid AJ, Colas D, de la Torre-Ubieta L, Zhu RP, Morgan AA, Santo EE, Ucar D, Devarajan K, Cole CJ, *et al*: FoxO6 regulates memory consolidation and synaptic function. Genes Dev 26: 2780-2801, 2012.
28. Chung SY, Huang WC, Su CW, Lee KW, Chi HS, Lin CT, Chen ST, Huang KM, Tsai MS, Yu HP and Chen SL: FoxO6 and PGC-1α form a regulatory loop in myogenic cells. Biosci Rep 33: e00045, 2013.
29. Sun Z, da Fontoura CSG, Moreno M, Holton NE, Sweat M, Sweat Y, Lee MK, Arbon J, Bidlack FB, Thedens DR, *et al*: FoxO6 regulates hippo signaling and growth of the craniofacial complex. PLoS Genet 14: e1007675, 2018.
30. Livak KJ and Schmittgen TD: Analysis of relative gene expression data using real-time quantitative PCR and the 2-(-Delta Delta C(T))method. Methods 25: 402-408, 2001.
31. Eley HL, Russell ST and Tisdale MJ: Mechanism of attenuation of muscle protein degradation induced by tumor necrosis factor-alpha and angiotensin II by beta-hydroxy-beta-methylbutyrate. Am J Physiol Endocrinol Metab 295: E1417-E1426, 2008.
32. Chen X, Wu Y, Yang T, Wei M, Wang Y, Deng X, Shen C, Li W, Zhang H, Xu W, *et al*: Salidroside alleviates cachexia symptoms in mouse models of cancer cachexia via activating mTOR signalling. J Cachexia Sarcopenia Muscle 7: 225-232, 2016.
33. Mandai S, Mori T, Nomura N, Furusho T, Arai Y, Kikuchi H, Sasaki E, Sohara E, Rai T, Uchida S, *et al*: WNK1 regulates skeletal muscle cell hypertrophy by modulating the nuclear localization and transcriptional activity of FOXO4. Sci Rep 14: 9101, 2018.
34. Derde S, Hermans G, Derese I, Güiza F, Hedström Y, Wouters PJ, Bruyninckx F, D'Hoore A, Larsson L, Van den Berghe G and Vanhorebeek I: Muscle atrophy and preferential loss of myosin in prolonged critically ill patients. Crit Care Med 40: 79-89, 2012.
35. Banduseela V, Ochala J, Lamberg K, Kalimo H and Larsson L: Muscle paralysis and myosin loss in a patient with cancer cachexia. Acta Myol 26: 136-144, 2007.
36. Risson V, Mazelin L, Roceri M, Sanchez H, Moncollin V, Corneloup C, Richard-Bulteau H, Vignaud A, Baas D, Defour A, *et al*: Muscle inactivation of mTOR causes metabolic and dystrophin defects leading to severe myopathy. J Cell Biol 187: 859-874, 2009.